

# Theoretical and X-ray Crystallographic Evidence of a Fluorine-Imine *Gauche* Effect: An Addendum to Dunathan's Stereoelectronic Hypothesis

Christof Sparr,<sup>[a]</sup> Evdokiya Salamanova,<sup>[b]</sup> W. Bernd Schweizer,<sup>[a]</sup>  
Hans Martin Senn,<sup>\*[b]</sup> and Ryan Gilmour<sup>\*[a]</sup>

**Abstract:** The preference of  $\beta$ -fluoroimines to adopt a *gauche* conformation has been studied by single-crystal X-ray diffraction analysis and DFT methods. Empirical and theoretical evidence for a preferential *gauche* arrangement around the NCCF torsion angle ( $\phi$ ) is presented ((*E*)-2-fluoro-*N*-(4-nitrobenzylidene)ethanamine:  $\phi_{\text{NCCF}} = 70.0^\circ$ ). In the context of this study, the analysis of a pyridoxal-derived  $\beta$ -fluoroaldimine

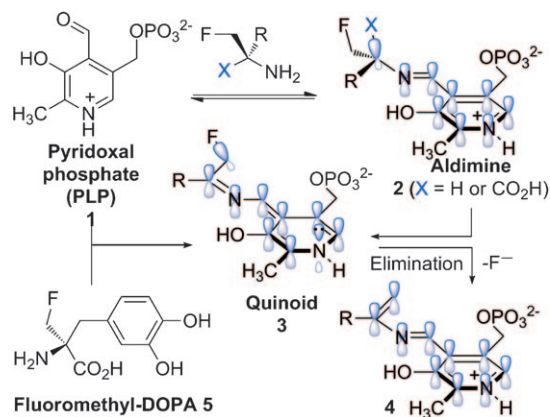
was performed, a species that is implicated in the inhibition of pyridoxal phosphate (PLP)-dependent enzymes by  $\beta$ -fluoroamine derivatives. The *gauche* preference of the internal aldimine (=NCH<sub>2</sub>CH<sub>2</sub>F) that can be ra-

tionalized by stereoelectronic arguments does not hold for the corresponding external system (N=CHCH<sub>2</sub>F) ( $E_{\text{min}}$  when  $\phi_{\text{NCCF}} = 120^\circ$ ). Moreover, the C–F bond is lengthened by more than 0.02 Å at  $\phi_{\text{NCCF}} = \pm 90^\circ$ , when it is exactly antiperiplanar to the conjugated imine. This activation of the C–F  $\sigma$  bond by an adjacent  $\pi$  system constitutes an addendum to Dunathan's stereoelectronic hypothesis.

**Keywords:** aldimines • conformation analysis • density functional theory • fluorine • *gauche* effect

## Introduction

Dunathan's stereoelectronic model to correlate the conformation and stereospecificity of pyridoxal phosphate (PLP **1**)-dependent enzymatic processes remains a milestone discovery in rationalizing the mechanistic intricacies of vitamin B<sub>6</sub> enzymes.<sup>[1]</sup> Of principal importance is the notion that  $\sigma$  bonds may be activated by an adjacent  $\pi$  system (Scheme 1). Consequently, the cofactor-derived Schiff bases **2** that are central to a plethora of enzyme mechanisms, including those of decarboxylases and racemases, share a common topological transition-state dependence on the  $\sigma$  bond being aligned with the  $\pi$ -system of the pyridoxal imine: in essence, maximum  $\sigma$ - $\pi$  overlap regulates reaction specificity.<sup>[2]</sup> Unsurprisingly, this mechanistic understanding has led to the rational design of numerous small molecule inhibitors for the treatment of neurodegenerative diseases, as well as PET imaging agents.<sup>[3,4]</sup> Many of these pharmaceuticals are fluorinated at the  $\beta$  position such that elimination from the transient quinoid intermediate **3** generates an



Scheme 1. The Dunathan hypothesis to correlate reaction specificity and conformation in PLP-dependent enzymes.<sup>[1]</sup>

electron sink **4**, which can covalently modify the enzyme active site, thus rendering it inactive. Pertinent examples of pharmaceuticals that exploit this design approach include  $\alpha$ -fluoromethyl-DOPA (**5**),  $\alpha$ -difluoromethyl-DOPA and related medicinally important compounds.<sup>[5,6]</sup>

Despite the wealth of literature pertaining to the reactivity and conformational dynamics of pyridoxal-derived Schiff bases,<sup>[7]</sup> including  $\beta$ -fluoroimines,<sup>[8]</sup> an important conformational issue remains unaddressed: do  $\beta$ -fluoroimines preferentially adopt a *gauche* conformation in a manner consistent with other fluorinated compounds containing a vicinal electron-withdrawing substituent?<sup>[9,10]</sup> Herein, we describe the synthesis and solid state analysis of three representative  $\beta$ -fluoroimines (**6–8**), including a vitamin B<sub>6</sub>-derived aldimine **8**, and quantify the empirical findings by theoretical methods. In view of the prominent role that  $\beta$ -fluoroamines have

[a] C. Sparr, Dr. W. B. Schweizer, Prof. Dr. R. Gilmour  
Swiss Federal Institute of Technology (ETH) Zürich  
Laboratory for Organic Chemistry  
Department of Chemistry and Applied Biosciences  
Wolfgang-Pauli-Str. 10, 8093 Zürich (Switzerland)  
E-mail: ryan.gilmour@org.chem.ethz.ch

[b] E. Salamanova, Dr. H. M. Senn  
WestCHEM and School of Chemistry  
University of Glasgow  
Glasgow G12 8QQ, Scotland (UK)  
Fax: (+44) 141-330-4888  
E-mail: senn@chem.gla.ac.uk

Supporting information for this article is available on the WWW under <http://dx.doi.org/10.1002/chem.201100644>.

historically played in the study and inhibition of PLP-dependent enzymes, this study is placed in the context of a wider theoretical conformational analysis of the transient intermediates involved. The conformational preferences of representative aldimine and quinoid intermediates are described together with a study of C–F activation as a function of  $\phi_{\text{NCCF}}$ .

## Results and Discussion

### Experimental structures in the solid state

As a start point for this study,  $\beta$ -fluoroimines **6–8** were prepared under dehydrative conditions from the corresponding aldehyde and 2-fluoroamine, and then evaluated by single-crystal X-ray diffraction analysis (Figure 1). Imine **6**, derived

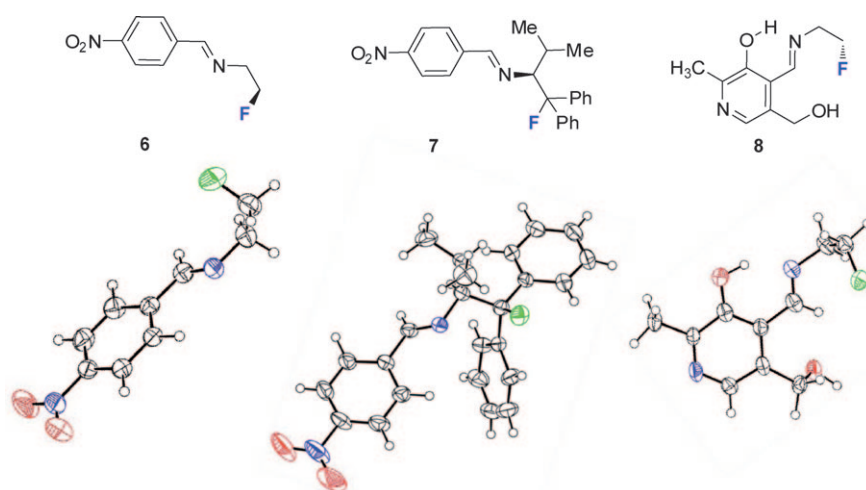


Figure 1. X-ray structures of  $\beta$ -fluoroimines **6**, **7** and **8**.<sup>[11–13]</sup>

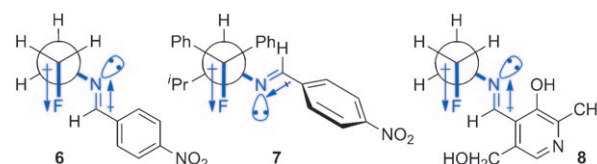
from 2-fluoroethylamine and *p*-nitrobenzaldehyde (Figure 1, left), in which there are no dominant steric interactions, crystallizes in the orthorhombic space group  $Pna2_1$ .<sup>[11]</sup> While the interatomic distances and angles are within the expected range, a clear *gauche* conformation is observed between the fluorine and nitrogen centres ( $\phi_{\text{NCCF}} = \pm 70.0^\circ$ ). Interestingly, the planar section of the  $\beta$ -fluoroimine **6** forms a  $\pi$ – $\pi$  interaction at a distance of 3.4 Å with a neighboring molecule translated along the *c* axis.

To compare this structural analysis with that of a more sterically demanding system, the valine-derived  $\beta$ -fluoroimine **7** was prepared (Figure 1, centre). This  $\beta$ -fluoroimine crystallizes in the polar space group  $C222_1$  with the fluorine adopting a *gauche* orientation relative to the imine nitrogen ( $\phi_{\text{NCCF}} = -74.2^\circ$ ). The nitrobenzyl group is rotated out of the imine plane ( $\phi_{\text{NCC}} = -25.5^\circ$ ),<sup>[12]</sup> likely induced by crystal packing forces where  $\pi$ – $\pi$  stacking with an adjacent nitrobenzyl moiety (distance of the two ring centroids = 3.75 Å) is the most dominant interaction. Finally, our attention was focussed on preparing and analyzing the pyridoxal-derived

$\beta$ -fluoroimine **8** (Figure 1, right); a species that is structurally analogous to the transient intermediates implicated in the disruption of many PLP-dependent enzymatic processes (**2**, Scheme 1). Analysis of the solid-state structure of this aldimine **8** reveals a racemic and an enantiomerically pure form.<sup>[13]</sup> Both forms have two symmetry-independent molecules in the asymmetric unit within the centrosymmetric triclinic space group  $P\bar{1}$  and the polar triclinic space group  $P1$ , respectively. Importantly, a clear *gauche* effect is observed ( $\phi_{\text{NCCF}} = \pm 67^\circ$ ). The orthogonal orientation of the (normally phosphorylated) primary hydroxyl group relative to the pyridine ring is also noteworthy, and all chemically intuitive hydrogen-bonding patterns are satisfied. It is important to note that in all cases the (*E*)-configured imines were isolated exclusively, thus minimizing steric stress, and that the non-sterically congested systems (**6** and **8**) adopt conformations in which the nitrogen lone pair points away from the fluorine atom to minimize electronic repulsion. Whereas the solid state conformations of **6** and **8** clearly show opposing C–F and C–N dipoles, this observation does not hold true for  $\beta$ -fluoroimine **7**, in which the nitrogen lone pair and the C–F bond are parallel (Scheme 2).

### Conformational analysis

*Conformational preferences of  $\beta$ -fluoroimines:* In an attempt to quantify the *gauche* conformational preference of the  $\beta$ -fluoroethylimines described in Figure 1, we embarked upon a



Scheme 2. Newman projections of  $\beta$ -fluoroimines **6**, **7** and **8**.

theoretical study of related systems at the DFT level. Initially, the NCCF bond rotational profile of the imine derived from  $\beta$ -fluoroethylamine and acetaldehyde was calculated in the vacuum and compared with the corresponding de-halogenated system (Figure 2; Table 1, entries 1–6). The parent system shows the usual symmetric rotation profile with three equivalent minima separated by barriers of about 13 kJ mol<sup>−1</sup>.

In the  $\beta$ -fluoro system (Table 1, entries 4–6), the symmetry of the bond rotational profile is broken, with the *−gauche* conformer being the most stable, followed by *anti* (+4 kJ mol<sup>−1</sup> relative to *−gauche*) and *+gauche*

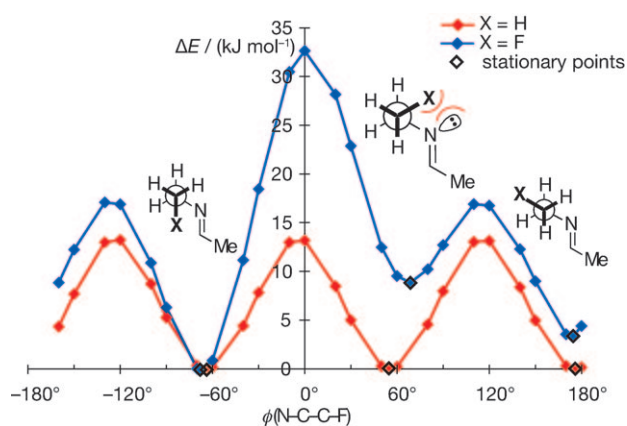


Figure 2. Bond-rotation profiles of acetaldehyde-derived imines (F vs. H), calculated in vacuum at the M06-2X/6-311G(2df,p) level.

Table 1. Calculated relative conformational energies and torsion angles of ethylimines derived from selected aldehydes RCHO.<sup>[a]</sup>

Entry	X	R	Conformer	$\Delta E$ [kJ mol <sup>-1</sup> ]	$\phi(\text{NCCX})$ [°]
1	H	Me	-gauche	0	-64
2	H	Me	+gauche	0	55
3	H	Me	anti	0	176
4	F	Me	-gauche	0	-68
5	F	Me	+gauche	9	69
6	F	Me	anti	4	175
7	F	H	-gauche	0	-68
8	F	H	+gauche	8	69
9	F	H	anti	4	175
10	F	4-NO <sub>2</sub> Ph (6)	-gauche	0	-67
11	F	4-NO <sub>2</sub> Ph (6)	+gauche	8	68
12	F	4-NO <sub>2</sub> Ph (6)	anti	6	176
13	F	4-MeOPh	-gauche	0	-68
14	F	4-MeOPh	+gauche	8	68
15	F	4-MeOPh	anti	3	176

[a] Results obtained with M06-2X/6-311G(2df,p) in vacuum.

(+9 kJ mol<sup>-1</sup>). An explanation for the preference of -gauche over anti is a stabilizing hyperconjugative  $\sigma_{\text{C-H}} \rightarrow \sigma^*_{\text{C-F}}$  interaction. To maximize the stabilizing overlap between the strongly electron-accepting  $\sigma^*_{\text{C-F}}$  orbital and the donating vicinal  $\sigma_{\text{C-H}}$  orbital (which is a better donor than  $\sigma_{\text{C-N}}$ ), the C-F bond is oriented anti to either vicinal C-H bond. Consequently, there is a stereoelectronic preference for the C-F bond being gauche to C-N. This deviation from simple steric and electrostatic arguments is known as the stereoelectronic "gauche effect", which is epitomized by 1,2-difluoroethane.<sup>[14]</sup> However, the gauche effect does not differentiate between the two possible gauche conformers ( $\pm g$ ). The observed destabilization of the +gauche conformer in the  $\beta$ -fluoroimines investigated here is a possible consequence of the overriding electrostatic repulsion between the imine and fluorine lone pairs, as schematically indicated in Figure 2. Qualitatively and quantitatively similar behavior has previously been reported for other systems containing fluorine in the  $\beta$  position with respect to a lone-pair-bearing heteroatom, such as  $\beta$ -fluoroamines or  $\beta$ -fluoroalcohols.<sup>[9c,f,h]</sup> The preferred -gauche minimum is protected by barriers of around 33 kJ mol<sup>-1</sup> (-gauche  $\rightarrow$  +gauche) and around

17 kJ mol<sup>-1</sup> (-gauche  $\rightarrow$  anti); the anti  $\rightarrow$  +gauche barrier is about 13 kJ mol<sup>-1</sup>. These energetic data suggest that all three conformers are accessible in equilibrium at 298 K, with relative populations of 1:0.2:0.03 (-gauche/anti/+gauche).

Based on the electronic origin of the preference for -gauche over anti, a dependence on the electronic nature of the imine is expected: the anti conformer should be the more disfavored the more electron-withdrawing the imine. To test this hypothesis, we investigated related  $\beta$ -fluoroimines derived from selected aldehydes RCHO (R=H, 4-NO<sub>2</sub>Ph (6), 4-MeOPh); see Table 1, entries 7–15. The comparison revealed only a small effect of the R group on the conformational preference of the  $\beta$ -fluoroimines. The stabilization of -gauche over anti is slightly more pronounced (6 vs. 3 kJ mol<sup>-1</sup>) for the electron-deficient aromatic imine (R=4-NO<sub>2</sub>Ph, Table 1, entries 10–12) as compared with the electron-rich species (R=4-MeOPh, Table 1, entries 13–15). Albeit small, this effect is consistent with the stereoelectronic explanation of the gauche effect, whereby the anti arrangement of acceptor bonds is disfavored. In all cases, the order of stability remains constant: -gauche < anti < +gauche.

**Natural bond orbital analyses:** The extent of the stereoelectronic gauche effect can be quantified by considering the stabilization gained from the hyperconjugative donor-acceptor interaction. Within the framework of the natural bond orbital (NBO) approach,<sup>[15]</sup> the interaction energy due to the delocalization of electron density from a donor NBO to an acceptor NBO can be calculated from a second-order perturbation theory expression. NBOs are localized orbitals constructed such as to provide the most accurate Lewis-like bonding picture, based on a given *N*-electron density, which can be obtained from any electronic-structure method. Specifically, for the case of the NCCF torsion, the NBO method yields localized bonding and anti-bonding NBOs for the C-F, C-H, and C-N bonds, and it quantifies the energy due to any donor-acceptor interactions between them.

In agreement with previous studies,<sup>[9f,h]</sup> it was found that the total donor-acceptor stabilization within the NCH<sub>2</sub>CH<sub>2</sub>F fragment is dominated by interactions between anti-oriented vicinal bonds. The vicinal gauche interactions are minor and change little upon rotation; the geminal interactions, although significant, are unaffected by rotation. We therefore used the sum of the six vicinal anti donor-acceptor interaction energies as a measure for the hyperconjugative stabilization,  $E_{\text{deloc}}$ . For instance, for the three conformers of the 4-nitrobenzaldimine 6,  $E_{\text{deloc}}$  amounts to -66, -64 and -57 kJ mol<sup>-1</sup> for the -gauche, +gauche and anti conformers, respectively. In the gauche conformers, the single largest contributor is indeed the  $\sigma_{\text{C-H}} \rightarrow \sigma^*_{\text{C-F}}$  interaction, which is worth about -20 kJ mol<sup>-1</sup>. In 6, the stereoelectronic preference for -gauche over anti is therefore  $\Delta E_{\text{deloc}}(-g, a) = -8.5$  kJ mol<sup>-1</sup>.

For the 4-methoxybenzaldimine, we expected less stereoelectronic stabilization, in line with the slightly smaller

*gauche* preference, due to the less electron-withdrawing nature of the imine. However,  $\Delta E_{\text{deloc}}(-g, a) = -8.2 \text{ kJ mol}^{-1}$  for the 4-methoxybenzalimine, insignificantly different from **6**, which hence cannot account for the difference in *gauche* preference. We therefore inspected the atomic partial charges derived from the NBO procedure. They are essentially independent of the torsional conformation.

However, in the *gauche* conformers, the two electronegative atoms F and N, which also bear negative NBO charges, are relatively close to one another ( $\approx 2.85 \text{ \AA}$ ). On electrostatic grounds, the *gauche* conformers are thus destabilized relative to the *anti* conformer. Whereas the NBO charge on fluorine is the same in both benzalimines ( $q_{\text{F}} = -0.40e$ ), the imine nitrogen is slightly more negatively charged in the more electron-rich 4-methoxy derivative ( $q_{\text{N}} = -0.48e$ ) than in the 4-nitro derivative **6** ( $q_{\text{N}} = -0.45e$ ). This amounts to a difference in electrostatic repulsion of about  $5 \text{ kJ mol}^{-1}$  (also considering the small change in the F–N distance, which is  $0.02 \text{ \AA}$  shorter in **6**). The larger *gauche* preference in **6** compared with the 4-methoxybenzalimine can thus be explained by a smaller electrostatic destabilization of the *gauche* conformer. It may therefore be concluded from this study that the electronic nature of the imine (electron rich vs. electron deficient) does have an effect, albeit small, on the NCCF torsional preference of  $\beta$ -fluoroimines. The *gauche* effect is slightly more pronounced in electron-poor imines. However, the reason for this is not the larger hyperconjugative stabilization, but the reduced electrostatic repulsion between the two electronegative atoms F and N.

**Conformational preferences of  $\beta$ -fluoropyridoximine:** For the pyridoximine **8**, we first considered the relative stabilities of the possible tautomeric forms with overall neutral charge, **8a–d** (Table 2). The focus on neutral forms was motivated two-fold: Firstly, our structural studies reported above have been limited to neutral  $\beta$ -fluoroimines. Secondly, recent detailed NMR spectroscopic investigations by Limbach and co-workers<sup>[16]</sup> have shown that the pyridine nitrogen of PLP aldimines is not protonated in aqueous solution near neutral pH ( $pK_{\text{a}} = 5.8$ ). This contrasts with the situation for PLP itself, which is N-protonated under the same conditions

( $pK_{\text{a}} = 8.2$ ). We therefore restricted ourselves to studying overall neutral forms of **8** as they are prevailing in physiological solutions, and considered a systematic study of the cations, which may well be relevant inside enzyme active sites, to be outside the scope of the present work.

In both vacuum and water, the enol-imine form **8a** is preferred. This is in agreement with the X-ray structure of **8** (Figure 3), which was unambiguously identified with the enol-imine form **8a** by comparing computed with experimental structural parameters. The keto–enamine tautomer **8b** is energetically competitive in water, where its equilibrium concentration amounts to about 0.5% at 298 K. The quinoid tautomer **8c** and the zwitterion **8d**, however, are only present in vanishingly small amounts under equilibrium conditions in either medium. As expected, the zwitterion is strongly stabilized in the polar solvent as compared with vacuum. For the low-energy tautomers **8a,b** as well as for the mechanistically important quinoid **8c**, we calculated NCCF bond rotation profiles in water (Figure 3 and Figure 4) and optimized the torsional conformers (in both vacuum and water; Table 3).

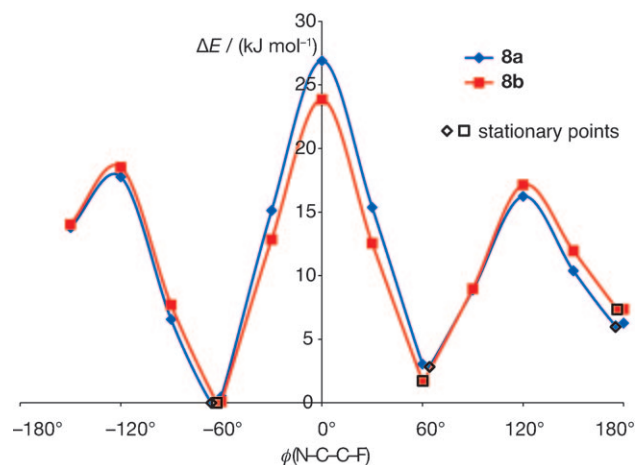


Figure 3. Bond-rotation profiles of  $\beta$ -fluoropyridoximine tautomers **8a** and **8b**, calculated in water at the M06-2X/6-31+G(d,p) level. Relative energies of stationary points using the larger 6-311G(2df, p) basis set differ by  $1 \text{ kJ mol}^{-1}$  (data not shown).

Table 2. Calculated relative stabilities of tautomeric and protonation forms of neutral pyridoximine **8** in vacuum and water.<sup>[a]</sup>

		(-g)- <b>8a</b>	(-g)- <b>8b</b>	(E)- <b>8c</b>	(Z)- <b>8c</b>	(-g)- <b>8d</b>
$\Delta E$ [kJ mol <sup>-1</sup> ]	vacuum	0	27	76 (-ac)	79 (anti)	115
	water	0	13	67 (syn)	71 (anti)	65

[a] Relative energies of the most stable conformer of each form at the M06-2X/6-311+G(2df,p) level in vacuum and continuum water, respectively.

Focussing on **8a,b** (Figure 3; Table 3, entries 1–6), we first note that their torsional preferences are essentially identical. Comparing **8a,b** in vacuum to the  $\beta$ -fluoroacetalimine (Figure 2; Table 1, entries 4–6) and the  $\beta$ -fluorobenzalimines (Table 1, entries 10–15) discussed above, the most obvious difference is the stabilization of the +*gauche* conformer, making the *anti* conformer now the least stable one. The order of stability for  $\beta$ -fluoropyridoximine **8** is therefore: -*gauche* < +*gauche* < *anti*. The energy of the *anti* relative to -*gauche* in **8a,b** is, however, the same as for the electron-deficient imine **6**.

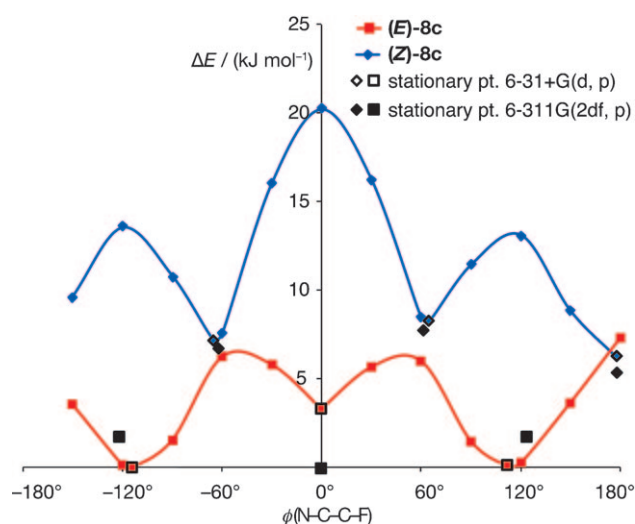


Figure 4. Bond-rotation profiles of the quinoid  $\beta$ -fluoropyridoximine tautomers (*E*)- and (*Z*)-**8c**, calculated in water at the M06-2X/6-31+G(d, p) level. Data for both isomers are plotted relative to the lowest stationary point at this level of theory, (*-ac*)-(*E*)-**8c**. Full black symbols show conformer energies obtained with the larger 6-311G (2df, p) basis set, relative to the lowest stationary point at that level, which is (*syn*)-(*E*)-**8c**.

Table 3. Calculated relative conformational energies of different forms of  $\beta$ -fluoropyridoximine **8**.<sup>[a]</sup>

Entry	Form	Conformer	$\Delta E$ [kJ mol <sup>-1</sup> ]	$\phi$ (NCCF) [°]
1	<b>8a</b>	- <i>gauche</i>	0 (0)	-66 (-65)
2	<b>8a</b>	+ <i>gauche</i>	6 (3)	64 (62)
3	<b>8a</b>	<i>anti</i>	6 (7)	176 (176)
4	<b>8b</b>	- <i>gauche</i>	0 (0)	-63 (-61)
5	<b>8b</b>	+ <i>gauche</i>	4 (2)	62 (60)
6	<b>8b</b>	<i>anti</i>	6 (8)	176 (176)
7	( <i>E</i> )- <b>8c</b>	- <i>ant</i> iclin	0 (2)	-133 (-123)
8	( <i>E</i> )- <b>8c</b>	+ <i>ant</i> iclin	0 (2)	135 (124)
9	( <i>E</i> )- <b>8c</b>	<i>syn</i>	2 (0)	0 (0)
10	( <i>Z</i> )- <b>8c</b>	- <i>gauche</i>	9 (6)	-62 (-62)
11	( <i>Z</i> )- <b>8c</b>	+ <i>gauche</i>	9 (8)	61 (61)
12	( <i>Z</i> )- <b>8c</b>	<i>anti</i>	3 (5)	179 (178)

[a] Results obtained with M06-2X/6-311G(2df,p) in vacuum and in continuum water (values in parentheses). Energies are relative to the most stable conformer of the respective form in vacuum or water, respectively.

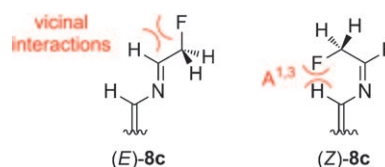
The stabilization of the +*gauche* conformer in **8a,b** is readily understood when one considers that the nitrogen lone pair is now accepting a hydrogen bond (**8a**) or is part of the conjugated system (**8b**). Repulsion with the fluorine lone pairs, responsible for the +*gauche* destabilization, is therefore significantly reduced. Otherwise, **8a,b** show qualitatively and quantitatively very similar conformational preferences to the previous  $\beta$ -fluoroimines. The NBO-derived stereoelectronic preference in favor of -*gauche* is  $\Delta E_{\text{deloc}}(-g, a) = -8.7$  kJ mol<sup>-1</sup> for **8a**, compared with  $-8.5$  kJ mol<sup>-1</sup> for **6**.

The net effect of solvation in **8a,b** is to stabilize the +*gauche* conformer and destabilize the *anti* relative to -*gauche*, however without changing the order of stability. The *anti* destabilization is in agreement with an enhanced stereoelectronic preference;  $\Delta E_{\text{deloc}}(-g, a) = -10.1$  kJ mol<sup>-1</sup> for **8a** in solution, compared with  $-8.7$  kJ mol<sup>-1</sup> in vacuum.

The stabilization of the +*gauche* conformer in **8a** results from a stronger hydrogen bond in solution; the OH...N distance reduces by 0.03–0.05 Å upon solvation, which further mitigates the lone-pair repulsion.

The quinoid tautomer **8c** can exist as two stereoisomers with respect to the configuration about the external (N=C<sub>α</sub>) imine double bond. Depending on which of the two C<sub>α</sub> protons in **8a** is abstracted, either (*E*)- or (*Z*)-**8c** is formed. The most stable conformer of the *E* isomer is always preferred (by about 4 kJ mol<sup>-1</sup>) to the most stable conformer of the *Z* isomer (Table 3, entries 7–12; Figure 4). It is important to note that the central bond of the NCCF torsion in **8c** is sp<sup>2</sup>-sp<sup>3</sup>, rather than sp<sup>3</sup>-sp<sup>3</sup> as in all the previous cases. This creates a different steric and stereoelectronic environment, thus we can expect torsional preferences to differ from the previously discussed systems.

The rotational profile for the less favored (*Z*)-**8c** (Figure 4) is still similar to **8a,b** in that the minima are at  $\phi_{\text{NCCF}} \approx \pm 60^\circ$  and  $180^\circ$ . However, the most stable conformer is now *anti*; and especially in water, the energy differences between the conformers are small (<3 kJ mol<sup>-1</sup>). This is consistent with an electrostatic control (repulsion between N and F), which favors *anti*; in water, the electrostatic interaction is screened, thus the differences between conformers are reduced. No stereoelectronic *gauche* preference is operational in this system. The barriers separating the minima are significantly lower in (*Z*)-**8c** than in **8a,b**, especially the central -*gauche* → +*gauche* barrier, which is almost halved. The rotational barriers in (*Z*)-**8c** are not caused by *syn*-vicinal interactions, but by relatively weak 1,3-allylic (A<sup>1,3</sup>) strain between the fluoromethyl group and the vinylic CH (Scheme 3).



Scheme 3. Unfavorable interactions responsible for the highest NCCF rotational barrier in (*E*)- and (*Z*)-**8c**, respectively.

Finally, in (*E*)-**8c** the NCCF rotation is almost unhindered, and the conformers are essentially energetically degenerate in both vacuum and water. Most notable is the interchange between minima and maxima in the torsional profile for (*E*)-**8c** as compared with all previous cases. The conformers of (*E*)-**8c** are at  $\phi_{\text{NCCF}} \approx \pm 120^\circ$  and  $0^\circ$ , whereas  $\phi_{\text{NCCF}} \approx \pm 60^\circ$  and  $180^\circ$  correspond to (low) barriers. The barriers are caused by unfavorable *syn*-vicinal interactions (Scheme 3). These are, however, much weaker than in, for example, **8a**, due to the wider sp<sup>2</sup> bond angle at C<sub>α</sub> (N-C<sub>α</sub>-C<sub>β</sub> is 131° in **8c**, but 111° in **8a**), which positions the terminal atoms of the NCCF torsion further apart (2.93 Å in **8c** vs. 2.57 Å in **8a** at  $\phi_{\text{NCCF}} = 0^\circ$ ). The flatness of the potential energy surface for NCCF rotation in (*E*)-**8c** is also reflected

in the relatively large influence of basis set and solvation on relative energies (several  $\text{kJ mol}^{-1}$ ) and exact positions of the minima ( $\approx 10^\circ$ ).

**C–F activation in  $\beta$ -fluoropyridoximines:** Returning to Dunathan's stereoelectronic hypothesis, we finally analyzed the effect of the NCCF torsion angle on the activation of the C–F bond in the quinoid (*E*)-**8c**. As a simple measure of C–F activation, the C–F bond length as a function of  $\phi_{\text{NCCF}}$  was determined (Figure 5). The C–F bond is lengthened by

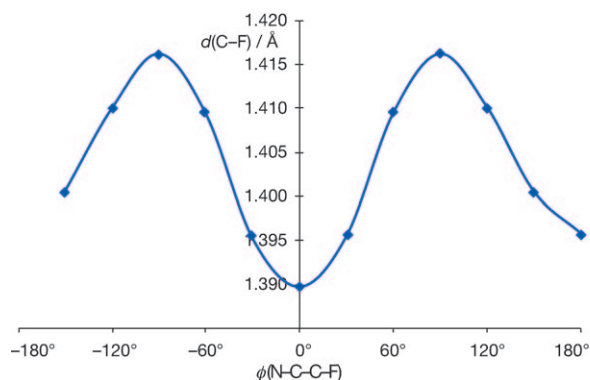


Figure 5. Variation of the C–F bond length with NCCF torsion in (*E*)-**8c**, calculated using M06-2X/6-31+G(d, p) in continuum water.

more than  $0.02 \text{ \AA}$  at  $\phi_{\text{NCCF}} = \pm 90^\circ$ , when it is exactly coplanar with the imine  $\pi$  system, compared with the *syn* conformer, when it is perpendicular to the  $\pi$  system. In the two anticlinal conformers ( $\phi_{\text{NCCF}} \approx \pm 120^\circ$ ), the C–F bond is almost as elongated as at  $\phi_{\text{NCCF}} = \pm 90^\circ$ . The NBO analysis revealed that there is indeed substantial  $\pi_{\text{N=C}} \rightarrow \sigma_{\text{C-F}}^*$  donation when the C–F bond is co-planar with the  $\pi$ -system. The antibonding  $\sigma_{\text{C-F}}^*$  orbital has an occupancy of  $0.05e$ , which weakens the C–F bond. In that conformation, the overlap between the donor and acceptor NBOs is optimal (Figure 6). The energy gained from this donor–acceptor interaction ( $-38 \text{ kJ mol}^{-1}$ ) is second only to the contributions from delocalization within the  $\pi$  system itself. Contrastingly, in the *syn* conformer, the C–F bond is antiperiplanar to the  $\text{C}_\alpha\text{–H}$  bond, which results in a much weaker  $\sigma_{\text{C-H}} \rightarrow \sigma_{\text{C-F}}^*$  interaction. The  $\sigma_{\text{C-F}}^*$  orbital is occupied by only  $0.01e$ , and the delocalization energy amounts to  $-15 \text{ kJ mol}^{-1}$ .

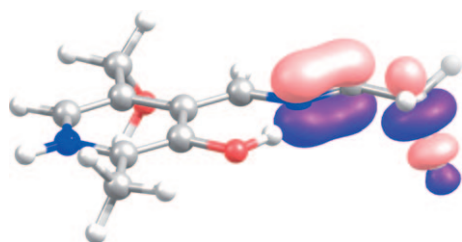


Figure 6. Illustration of the stereoelectronic C–F activation in (*E*)-**8c** at  $\phi_{\text{NCCF}} = 90^\circ$ . Shown are the occupied  $\pi_{\text{N=C}}$  and the vacant  $\sigma_{\text{C-F}}^*$  NBOs.

Therefore in the *E*-quinoid the stereoelectronic situation is such that the C–F bond (or any other acceptor bond) is preferentially activated when it is aligned with the extended  $\pi$  system. Moreover, this conformation is accessible at very little energetic cost as the NCCF rotation is practically unhindered, accounting for the facile elimination of fluoride from the transient quinoid species to generate the Michael acceptor that is necessary for inhibition of PLP-dependent enzymes by  $\beta$ -fluoroamine derivatives.

## Conclusion

We have presented theoretical and crystallographic evidence that  $\beta$ -fluoroimines preferentially adopt one of two possible *gauche* conformations, and that the overall order of stability is  $-gauche < anti < +gauche$ . A stereoelectronic rationale for this conformational preference is a stabilizing hyperconjugative interaction from the  $\sigma_{\text{C-H}}$  bond into the low lying  $\sigma^*$  orbital of the C–F bond ( $\sigma_{\text{C-H}} \rightarrow \sigma_{\text{C-F}}^*$ ).<sup>[14]</sup> In the context of this study, a theoretical approach has enabled us to compare and contrast the conformational preferences of both the “internal” (F–C–C–N=C) aldimine and “external” quinoid (F–C–C=N–C) intermediates that are implicated in the mechanism of PLP-dependent enzyme inhibition. The *gauche* preference of the “internal” aldimine ( $=\text{NCH}_2\text{CH}_2\text{F}$ ), which can be rationalized by stereoelectronic arguments, does not hold for the corresponding “external” system ( $\text{N}=\text{CHCH}_2\text{F}$ ) ( $E_{\text{min}}$  when  $\phi_{\text{NCCF}} = 0^\circ$ ). Moreover, the C–F bond is lengthened by more than  $0.02 \text{ \AA}$  at  $\phi_{\text{NCCF}} = \pm 90^\circ$ , when it is exactly orthogonal to the plane of the conjugated imine. This activation of the C–F  $\sigma$  bond by an adjacent  $\pi$  system is consistent with Dunathan's stereoelectronic model.

## Experimental Section

### Synthesis and structure determination:

See the Supporting Information for full experimental details.

**Data for 6:** Isolated as a yellow solid (m.p.  $102\text{--}103^\circ\text{C}$ );  $^1\text{H NMR}$  (400 MHz,  $\text{CDCl}_3$ ):  $\delta = 8.41$  (s, 1H; CHN), 8.27 (ddd,  $^3J = 8.9, 1.9, 1.9$  Hz, 2H;  $\text{CHCNO}_2$ ), 7.92 (ddd,  $^3J = 9.1, 2.0, 2.0$  Hz, 2H;  $\text{CHCCNO}_2$ ), 4.76 (dt,  $^2J_{\text{HF}} = 47.2, 4.9, 2\text{H}$ ;  $\text{CH}_2\text{F}$ ), 3.96 ppm (dt,  $^3J_{\text{HF}} = 28.8, 4.7, 2\text{H}$ ;  $\text{CH}_2\text{N}$ );  $^{13}\text{C NMR}$  (100 MHz,  $\text{CDCl}_3$ ):  $\delta = 161.3$  (CHN), 149.2 ( $\text{CNO}_2$ ), 141.3 (CCHN), 129.0 ( $\text{CCNO}_2$ ), 123.9 ( $\text{CCCNO}_2$ ), 82.4 (d,  $^1J_{\text{CF}} = 169.8$  Hz; CF), 61.3 ppm (d,  $^2J_{\text{CF}} = 19.8$  Hz, CCF);  $^{19}\text{F NMR}$  (376 MHz,  $\text{CDCl}_3$ ):  $\delta = -222.5$  ppm (tt,  $^2J_{\text{FH}} = 47.2, 28.6$  Hz); IR (neat):  $\tilde{\nu}_{\text{max}} = 3104$  (w), 2969 (w), 2903 (w), 1644 (m), 1603 (m), 1514 (s), 1433 (w), 1415 (w), 1392 (w), 1329 (s), 1290 (m), 1225 (m), 1104 (m), 1056 (m), 1028 (s), 1009 (m), 976 (w), 913 (m), 859 (s), 828 (s), 749 (m), 690 (m), 768 (w), 662  $\text{cm}^{-1}$  (w); HRMS (ESI):  $m/z$ : calcd for:  $\text{C}_9\text{H}_{10}\text{FN}_2\text{O}_2^+$ : 197.0721 [ $\text{MH}^+$ ]; found: 197.0714.

**Data for 7:** Isolated as an off white solid; m.p.  $147\text{--}148^\circ\text{C}$ ;  $[\alpha]_{\text{D}}^{20} + 118.2$  ( $c = 1.05$  in  $\text{CHCl}_3$ );  $^1\text{H NMR}$  (400 MHz,  $\text{CDCl}_3$ ):  $\delta = 8.19$  (ddd,  $^3J = 9.0, 2.0, 2.0$  Hz, 2H;  $\text{CHCNO}_2$ ), 7.84 (s, 1H; CHN), 7.71 (ddd,  $^3J = 9.0, 2.0, 2.0$  Hz, 2H;  $\text{CHCCNO}_2$ ), 7.61–7.67 (m, 2H; Ph), 7.35–7.43 (m, 2H; Ph), 7.14–7.31 (m, 6H; Ph), 3.76 (dd,  $^3J_{\text{HF}} = 22.0, 5.0$  Hz, 1H;  $\text{CHCF}$ ), 2.21–2.38 (m, 1H;  $\text{CHMe}_2$ ), 0.85–0.96 ppm (m, 6H; Me);  $^{13}\text{C NMR}$  (100 MHz,  $\text{CDCl}_3$ ):  $\delta = 160.1$  (CHN), 149.0 ( $\text{CNO}_2$ ), 142.6 (d,  $^2J_{\text{CF}} = 23.2$  Hz;  $\text{Ph}^1$ ), 141.4 (CCHN), 141.3 (d,  $^2J_{\text{CF}} = 22.7$  Hz;  $\text{Ph}^1$ ), 128.7

(CCNO<sub>2</sub>), 128.1 (Ph<sup>3</sup>), 127.9 (d, <sup>4</sup>J<sub>CF</sub>=1.6 Hz; Ph<sup>3</sup>), 127.6 (Ph<sup>4</sup>), 127.4 (Ph<sup>4</sup>), 126.1 (d, <sup>3</sup>J<sub>CF</sub>=10.3 Hz; Ph<sup>2</sup>), 125.8 (d, <sup>3</sup>J<sub>CF</sub>=9.3 Hz; Ph<sup>2</sup>), 123.8 (CCNO<sub>2</sub>), 100.8 (d, <sup>1</sup>J<sub>CF</sub>=185.4 Hz; CF), 83.6 (d, <sup>2</sup>J<sub>CF</sub>=23.9 Hz; CCF), 29.9 (CMe<sub>2</sub>), 21.6 (d, <sup>4</sup>J<sub>CF</sub>=3.3 Hz; Me), 19.3 ppm (d, <sup>4</sup>J<sub>CF</sub>=3.4 Hz; Me'); <sup>19</sup>F NMR (376 MHz, CDCl<sub>3</sub>): δ = -155.3 ppm (d, <sup>3</sup>J<sub>HF</sub>=20.3 Hz); IR (neat): ν<sub>max</sub>=2963 (w), 1645 (w), 1598 (m), 1517 (s), 1450 (m), 1338 (s), 1201 (w), 1145 (w), 1102 (w), 1061 (m), 993 (m), 941 (w), 882 (w), 856 (m), 789 (m), 757 (s), 747 (s), 696 (s), 668 (m), 638 cm<sup>-1</sup> (w); HRMS (ESI): m/z: calcd for C<sub>24</sub>H<sub>24</sub>FN<sub>2</sub>O<sub>2</sub><sup>+</sup>: 391.1816 [MH<sup>+</sup>]; found: 391.1824.

**Data for 8:** Isolated as a yellow solid; m.p. 140–141 °C; <sup>1</sup>H NMR (400 MHz, CDCl<sub>3</sub>): δ = 13.71 (brs, 1H; OH), 8.86 (s, 1H; CHN), 7.83 (s, 1H; CH<sub>py</sub>), 4.73 (s, 2H; CH<sub>2</sub>OH), 4.67 (dt, <sup>2</sup>J<sub>HF</sub>=47.3, 4.8 Hz, 2H; CH<sub>2</sub>F), 3.91 (dtd, <sup>3</sup>J<sub>HF</sub>=27.9, 4.7, 1.2 Hz, 2H; CH<sub>2</sub>N), 2.46 (s, 3H; CH<sub>3</sub>), 2.02 ppm (brs, 1H; OH); <sup>13</sup>C NMR (100 MHz, CDCl<sub>3</sub>): δ = 165.0 (CHN), 154.6 (C<sub>py</sub>), 151.0 (C<sub>py</sub>), 138.1 (C<sub>py(6)</sub>), 131.0 (C<sub>py</sub>), 119.8 (C<sub>py</sub>), 82.0 (d, <sup>1</sup>J<sub>CF</sub>=171.2 Hz; CF), 60.7 (CH<sub>2</sub>OH), 59.7 (d, <sup>2</sup>J<sub>CF</sub>=19.8 Hz; CCF), 19.0 ppm (CH<sub>3</sub>); <sup>19</sup>F NMR (376 MHz, CDCl<sub>3</sub>): δ = -222.9 ppm (tt, <sup>2</sup>J<sub>FH</sub>=47.1, 27.9 Hz); IR (neat) ν<sub>max</sub>=3126 m, 2836 (w), 1631 (s), 1403 (s), 1340 (m), 1294 (m), 1260 (m), 1211 (m), 1119 (w), 1085 (w), 1023 (s), 988 (w), 964 (w), 906 (w), 856 (s), 786 (w), 756 (w), 714 (m), 640 cm<sup>-1</sup>w; HRMS (ESI): m/z: calcd for C<sub>10</sub>H<sub>14</sub>FN<sub>2</sub>O<sub>2</sub><sup>+</sup>: 213.1034 [MH<sup>+</sup>]; found: 213.1034.

## Computational Details

All calculations were done with Gaussian 09<sup>[17]</sup> using DFT. The M06–2X hybrid meta-GGA exchange–correlation functional was used throughout, which has been shown to yield superior accuracy not only for main-group thermochemistry, but in particular for non-covalent interactions, including dispersion and hydrogen bonding.<sup>[18]</sup> Even though such interactions are not expected to be dominant in the systems studied here, they may well influence conformational preference. We used standard Pople-style basis sets, starting with 6-31+G(d,p), in which the addition of diffuse functions on non-hydrogen atoms enormously improves energetics when using DFT methods, comparable to what is achieved with triple-ζ basis sets.<sup>[19]</sup> Minima were re-optimized using 6-311G(2df, p) and spot-checked with 6-311+G(2df, p). Except for (*E*)-**8c**, the effect of basis set on relative energies was <1 kJ mol<sup>-1</sup>. Calculations in water solvent used the IEF-PCM polarizable continuum model with UFF atomic radii for the cavity construction. Non-electrostatic contributions to solvation were not included (which corresponds to the default solvation treatment in Gaussian 09). Default convergence criteria were applied for the SCF and in geometry optimizations. All stationary points were confirmed as minima by a positive-definite Hessian. Values for rotational barriers were estimated from the maxima of the torsion profiles.

## Acknowledgements

We gratefully acknowledge generous financial support from the Alfred Werner Foundation (assistant professorship to R.G.), the Roche Research Foundation, Novartis AG (doctoral fellowships to C.S.), and the ETH Zürich.

- [1] H. C. Dunathan, *Proc. Natl. Acad. Sci. USA* **1966**, *55*, 712–716.  
 [2] a) C. T. Walsh, *Enzymatic Reaction Mechanisms*, 2nd ed., W. H. Freeman, San Francisco, **1979**; b) J. C. Vederas, H. G. Floss, *Acc. Chem. Res.* **1980**, *13*, 455–463; c) H. Hayashi, H. Wada, T. Yoshimura, N. Esaki, K. Soda, *Annu. Rev. Biochem.* **1990**, *59*, 87–110; d) H. Hayashi, *J. Biochem.* **1995**, *118*, 463–473; e) A. C. Eliot, J. F. Kirsch, *Annu. Rev. Biochem.* **2004**, *73*, 383–415; f) T. D. H. Bugg in *Introduction to Enzyme and Coenzyme Chemistry*, 2nd ed., Wiley-Blackwell, New York, **2004**, pp. 211–226.  
 [3] C. T. Walsh, *Annu. Rev. Biochem.* **1984**, *53*, 493–535.

- [4] For examples, see a) B. Lippert, B. W. Metcalf, R. J. Resvick, *Biochem. Biophys. Res. Commun.* **1982**, *108*, 146–152; b) W. S. Faraci, C. T. Walsh, *Biochemistry* **1989**, *28*, 431–437; c) D. B. Berkowitz, K. R. Karukurichi, R. De La Salud-Bea, D. L. Nelson, C. D. McCune, *J. Fluorine Chem.* **2008**, *129*, 731–742; d) D. B. Berkowitz, K. R. Karukurichi, R. De La Salud-Bea, G. Maiti, J. M. McFadden, M. L. Morris, *ACS Symp. Ser.* **2009**, *1009*, 288–303; e) D. B. Berkowitz, R. de La Salud-Bea, W.-J. Jahng, *Org. Lett.* **2004**, *6*, 1821–1824.  
 [5] D. Murali, L. G. Flores, A. D. Roberts, R. J. Nickles, O. T. DeJesus, *Appl. Radiat. Isot.* **2003**, *59*, 237–243.  
 [6] M. G. Palfreyman, C. Danzin, P. Bey, M. J. Jung, G. Ribereau-Gayon, M. Aubry, J. P. Vevert, A. Sjoerdsma, *J. Neurochem.* **1978**, *31*, 927–932.  
 [7] For selected examples, see a) M.-D. Tsai, H. J. R. Weintraub, S. R. Byrn, C. Chang, H. G. Floss, *Biochemistry* **1978**, *17*, 3183–3188; L. Casella, M. Gullotti, *J. Am. Chem. Soc.* **1983**, *105*, 803–809; b) M. Nagata, M. Doi, M. Inoue, T. Ishida, M. Kamigauchi, M. Sugiura, A. Wakahara, *J. Chem. Soc. Perkin Trans. 2* **1994**, 983–988.  
 [8] a) C. Béguin, S. Hamman, *Org. Magn. Reson.* **1981**, *16*, 129–132; b) M. C. Salon, S. Hamman, C. G. Béguin, *Org. Magn. Reson.* **1983**, *21*, 265–270; c) M. C. Salon, S. Hamman, C. G. Béguin, *J. Fluorine Chem.* **1985**, *27*, 361–370; d) H. Ünver, E. Kendi, K. Güven, T. N. Durlu, *Z. Naturforsch. B* **2002**, *57*, 685–690.  
 [9] For selected examples, see a) D. O'Hagan, C. Bilton, J. A. K. Howard, L. Knight, D. J. Tozer, *J. Chem. Soc. Perkin Trans. 2* **2000**, 605–607; b) C. R. S. Briggs, D. O'Hagan, J. A. K. Howard, D. S. Yufit, *J. Fluorine Chem.* **2003**, *119*, 9–13; c) C. R. S. Briggs, M. J. Allen, D. O'Hagan, D. J. Tozer, A. M. Z. Slawin, A. E. Goeta, J. A. K. Howard, *Org. Biomol. Chem.* **2004**, *2*, 732–740; d) N. E. J. Gooseman, D. O'Hagan, A. M. Z. Slawin, A. M. Teale, D. J. Tozer, R. J. Young, *Chem. Commun.* **2006**, 3190–3192; e) N. E. J. Gooseman, D. O'Hagan, M. J. G. Peach, A. M. Z. Slawin, D. J. Tozer, R. J. Young, *Angew. Chem.* **2007**, *119*, 6008–6012; *Angew. Chem. Int. Ed.* **2007**, *46*, 5904–5908; f) D. Y. Buissonneaud, T. van Mourik, D. O'Hagan, *Tetrahedron* **2010**, *66*, 2196–2202; g) for an excellent review see D. O'Hagan, *Chem. Soc. Rev.* **2008**, *37*, 308–319; h) I. Hyla-Kryspin, S. Grimme, S. Hruschka, G. Haufe, *Org. Biomol. Chem.* **2008**, *6*, 4167–4175.  
 [10] For examples from this laboratory see a) C. Sparr, W. B. Schweizer, H. M. Senn, R. Gilmour, *Angew. Chem.* **2009**, *121*, 3111–3114; *Angew. Chem. Int. Ed.* **2009**, *48*, 3065–3068; b) C. Bucher, C. Sparr, W. B. Schweizer, R. Gilmour, *Chem. Eur. J.* **2009**, *15*, 7637–7647; c) C. Mondelli, C. Bucher, A. Baiker, R. Gilmour, *J. Mol. Catal. A: Chem.* **2010**, *327*, 87–91; d) C. Sparr, R. Gilmour, *Angew. Chem.* **2010**, *122*, 6670–6673; *Angew. Chem. Int. Ed.* **2010**, *49*, 6520–6523; e) C. Bucher, R. Gilmour, *Angew. Chem.* **2010**, *122*, 8906–8910; *Angew. Chem. Int. Ed.* **2010**, *49*, 8724–8728; f) S. Paul, W. B. Schweizer, M.-O. Ebert, R. Gilmour, *Organometallics* **2010**, *29*, 4424–4427.  
 [11] Selected crystallographic data for **6**: *M*<sub>r</sub>=196.181; orthorhombic *Pna*2<sub>1</sub>; *a*=10.3049(5), *b*=20.0536(12), *c*=4.4424(2) Å; *α*=90.00, *β*=90.00, *γ*=90.00°; *φ*<sub>NCCF</sub>=±70.0°.  
 [12] Selected crystallographic data for **7**: *M*<sub>r</sub>=390.458; orthorhombic *C222*<sub>1</sub>; *a*=8.0748(2), *b*=15.9339(4), *c*=31.8928(8) Å; *α*=90.00, *β*=90.00, *γ*=90.00°; *φ*<sub>NCCF</sub>=-74.2°; polar space group; configuration of the starting material known.  
 [13] Selected crystallographic data for **8**: *M*<sub>r</sub>=212.224; triclinic *P* $\bar{1}$ ; *a*=7.166(2), *b*=11.489(3), *c*=12.575(3); *α*=96.917(14), *β*=89.939(14), *γ*=101.869(13)°; *φ*<sub>NCCF</sub>=±67.0/±66.9°<sup>[a]</sup> triclinic *P1*; *a*=4.4723(1), *b*=10.1486(1), *c*=11.9847(2) Å; *α*=105.698(1), *β*=92.052(1), *γ*=96.745(1)°; *φ*<sub>NCCF</sub>=67.0°/66.3°<sup>[b]</sup> [a] Centrosymmetric space group with 2 symmetry independent molecules in the asymmetric unit. [b] Polar space group with two symmetry independent molecules in the unit cell, both gauche conformers observed.  
 [14] L. Goodman, H. B. Gu, V. Pophristic, *J. Phys. Chem. A* **2005**, *109*, 1223–1229.

- [15] F. Weinhold, C. R. Landis, *Valency and Bonding: A Natural Bond Orbital Donor–Acceptor Perspective*, Cambridge University Press, Cambridge, **2005**.
- [16] a) S. Sharif, M. C. Hout, P. M. Tolstoy, M. D. Toney, K. H. M. Jons-son, H.-H. Limbach, *J. Phys. Chem. B* **2007**, *111*, 3869–3876; b) M. Chan-Huot, C. Niether, S. Sharif, P. M. Tolstoy, M. D. Toney, H.-H. Limbach, *J. Mol. Struct.* **2010**, *976*, 282–289; c) M. Chan-Huot, S. Sharif, P. M. Tolstoy, M. D. Toney, H.-H. Limbach, *Biochemistry* **2010**, *49*, 10818–10830.
- [17] Gaussian 09, Revision A.02, M. J. Frisch, G. W. Trucks, H. B. Schlegel, G. E. Scuseria, M. A. Robb, J. R. Cheeseman, G. Scalmani, V. Barone, B. Mennucci, G. A. Petersson, H. Nakatsuji, M. Caricato, X. Li, H. P. Hratchian, A. F. Izmaylov, J. Bloino, G. Zheng, J. L. Sonnenberg, M. Hada, M. Ehara, K. Toyota, R. Fukuda, J. Hasegawa, M. Ishida, T. Nakajima, Y. Honda, O. Kitao, H. Nakai, T. Vreven, J. A. Montgomery, Jr., J. E. Peralta, F. Ogliaro, M. Bearpark, J. J. Heyd, E. Brothers, K. N. Kudin, V. N. Staroverov, R. Kobayashi, J. Normand, K. Raghavachari, A. Rendell, J. C. Burant, S. S. Iyengar, J. Tomasi, M. Cossi, N. Rega, J. M. Millam, M. Klene, J. E. Knox, J. B. Cross, V. Bakken, C. Adamo, J. Jaramillo, R. Gomperts, R. E. Stratmann, O. Yazyev, A. J. Austin, R. Cammi, C. Pomelli, J. W. Ochterski, R. L. Martin, K. Morokuma, V. G. Zakrzewski, G. A. Voth, P. Salvador, J. J. Dannenberg, S. Dapprich, A. D. Daniels, Ö. Farkas, J. B. Foresman, J. V. Ortiz, J. Cioslowski, D. J. Fox, Gaussian, Inc., Wallingford CT, **2009**.
- [18] a) Y. Zhao, D. G. Truhlar, *Theor. Chem. Acc.* **2008**, *120*, 215–241; b) Y. Zhao, D. G. Truhlar, *Acc. Chem. Res.* **2008**, *41*, 157–167.
- [19] B. J. Lynch, Y. Zhao, D. G. Truhlar, *J. Phys. Chem. A* **2003**, *107*, 1384–1388.

Received: February 28, 2011  
Published online: July 5, 2011